Synthesis and characterization of linear polyimides with intrinsic microporosity and their hydrogen adsorption studies

Fadi Ibrahim

Department of Chemistry, Abdul Latif Thanian Al-Ghanim School Kuwait.

ABSTRACT

A series of linear microporous polymers were successfully prepared by conventional nucleophilic substitution reaction of several newly synthesized tetrachloro-monomers with commercially available 5,5',6,6'-tetrahydroxy-3,3,3',3'-tetramethylspirobisindane. From the porosity analysis it is clear that the prepared polymers are analogous to polymers of intrinsic microporosity (PIMs) with high surface area (350-800 m^2/g). The *t*-plot analysis shown that the major contribution to the specific surface area is arising from the micropore surface area with narrow size distribution of ultramicropores as confirmed by the Horvath-Kawazoe (H-K) analysis. The hydrogen storage capacity of the prepared PIM-SI-(1-7)s were promising (up to 1.26 wt%, 77 K, at 1.13 bar) with high isoteric heats of H_2 adsorption (8.5 kJ/mol). The results of this study demonstrate that we can use cheaper chlorinated monomers (instead of fluoro-monomers) provide a uniform intrinsic microporous in the target polymers.

Introduction

Many approaches have been used to develop various insoluble network organic microporous polymers such as hyper cross-linked polymers (HCP)[1,2], triptycene-based PIM (Trip-PIM)[3], conjugated microporous polymers (CMP)[4], organic framework polymer (OFP)[5], porous organic polymers (POP)[6] and microporous polyimide networks[7] with high specific surface. It is important to note that if there is a certain amount of free volume, voids would be interconnected, and the polymer will therefore behave as a microporous material even without a network structure. This kind of microporous polymer could be soluble to facilitate easy solution-based processing which can't be achieved in other microporous materials. The porous properties mainly due to the architectural features of the used monomers which defines the microporosity. The combined features: high rigidity arising from dioxane linkages and the randomly contorted structure due to either a spiro-centre or a non-planar architecture, represent a prerequisite to induce space inefficient packing producing a large amount of interconnected free volume. The most outstanding representation for this kind of materials are the polymers of intrinsic microporosity (PIMs)[9] developed by McKeown and Budd et al with high surface areas in the range of 500-900 m^2/g. Typical example is PIM-**1**, prepared as a soluble polymer from the dioxane forming reaction between 5,5',6,6'-tetrahydroxy-3,3,3',3'-tetramethylspirobisindane and 4-dicyanotetraflurobenzene. The objective of the paper is to develop a new high surface area of soluble organic polymers, to study its potential utility in hydrogen, nitrogen storage and its related applications. Great interests in soluble, microporous polyimides[10] due to there are much easier to process than crosslinking polymers. However, only a very limited number of microporous, soluble polymers are known up to now.[11-15] This can be related to the high polymerization difficulty, which are posed onto polymer architecture in order to provide both high free volume and resistance against pore collapse. This paper investigates the influence of the molecular structure, reaction temperature,

K_2CO_3 and solvent effects on polymerization. It is important to focuses on the impact of polymer backbone architecture (kink as TTSBI monomer, angle, and monomer length as SI-(**1-7**)-4F, etc). Condensation of these monomers with TTSBI allows a tuning of the overall polymer flexibility and the spacing between the kinks along the polymer chain.

Experimental

Characterization

^{1}H-NMR spectrum (400 MHz) of monomers and polymers were recorded on a Bruker DPX 400 spectrometer using $CDCl_3$ as the solvent and tetramethylsilane as the internal standard. FT-IR spectra were recorded on a JASCO FT/IR-6300. Elemental analyses were carried out using Elementar Vario Micro Cube. Mass analyses were done on a Thermo DFS Mass spectrometer. The molecular weight and its distribution were measured by Knauer Gel Permeation Chromatograph fitted with a refractive index detector (flow rate 1 mL/min) according to polystyrene standards using $CHCl_3$ as the eluent. Thermogravimetric analysis (TGA) was performed with a Shimadzu TGA-50 instrument at a heating rate of 10 °C/min under nitrogen atmosphere and DSC analysis was done on Shimadzu DSC-60 instrument at a heating rate of 10 °C/min under nitrogen. Melting points were measured with a Griffin melting point apparatus and further confirmed by DSC analysis. Wide-angle X-ray diffraction (WAXD) of films was measured by a Siemens D5000 diffractometer. Microscopic techniques employed are Scanning Electron Microscopy (SEM: JEOL Model 6300) and High Resolution Transmission Electron Microscopy (HRTEM: JEOL Model JEM-3010).

Nitrogen adsorption measurements (77 K) and volumetric hydrogen adsorptions analysis (77 K and 87 K at 1.13 bar) were performed on a Micromeritics ASAP 2020 Sorptometer equipped with an out gassing platform, an online data acquisition and handling system. Before analysis the samples were degassed for 12 h with a heating rate of 1 °C/min in two stages (80 °C for 1 h and 120 °C for 11h) under high vacuum (< 10^{-4} mbar). The specific surface area was calculated using the

Tele:
E-mail addresses: fed_ooo@yahoo.com

Brunauer-Emmet-Teller (BET) equation. The micropore area was calculated using *t*-plot method. The pore size distributions were calculated from the adsorption isotherm using the Horvath-Kawazoe (H-K) calculations. The heats of adsorption were calculated from the hydrogen adsorption isotherms obtained at 77.3 K and 87 K using the ASAP 2020 software (Micromeritics, Norcross, GA).

Materials

The anhydrous solvents DMF and DMAc were purchased from Aldrich co, and the potassium carbonate obtained from Merck was finely grounded and dried at 200 $^{\circ}$C. 2,3,5,6-tetrafluoroterephthalonitrile obtained from aldrich was used directly. 5,5′,6,6′-tetrahydroxy-3,3,3′,3′-tetramethyl-1,1′-spirobisindane obtained from alfa was purified from methanol. Starting from dichlorophthalic acid, dichlorophthalic anhydride was prepared in our laboratory. The other commercially available materials and solvents were used without further purification.

Film Preparation

Polymer (550 mg) was dissolved in CHCl$_3$ (15 mL) and filtered (2 μm glass microfiber). The filtered solution was pouring into a flat Petri dish (12 cm dia.) and then placed in a vacuum dessicator with the gas inlet open to the atmosphere. The solution was allowed to evaporate for 4 days. The dish was removed and the clear yellow film released from the glass.

Synthesis of Soluble Imide Momoers (SI-4Cls)

1,5-bis-(5,6-Dichloro-Naphthalene)Isoindoline-1,3-Dione), (SI-1-4Cl)

A solid of 1,5-diaminonaphthalene (0.23 g, 1.45 mmol) was added gradually to a solution of dichlorophethalic anhydride (0.8 g, 3.70 mmol) in acetic acide (50 ml) at 100 $^{\circ}$C for 4 h. After cooling, the reaction mixture was poured into deionised water and the solid product (SI-1-4Cl) collected by filtration washed with *n*-hexane. The obtained white powder was dried in vacuum oven at 100 $^{\circ}$C for 12 h. Yield: 85%; m.p. 216 $^{\circ}$C; ^{1}H NMR (CDCl$_3$, 400 MHz, δ ppm): 8.03 (s, 4H), 7.15-7.18 (d, 2H), 6.53-6.50 (d, 2H), 6.32-6.29 (t, 2H). FTIR (KBr) υ/cm^{-1}: 3088, 1774 and 1723 (imide). CHN Calculated for C$_{26}$H$_{10}$Cl$_4$N$_2$O$_4$ (554): C, 63.93; H, 2.04; N, 5.73. Found: C, 63.29; H, 1.88; N, 5.02.

The following monomers were prepared from dichlorophthalic anhydride and corresponding amines using similar procedures adopted for (SI-1-4Cl).

1,4-bis-(5,6-dichloro-1,3-dioxoisoindolin-2-yl)-2,3,5,6-tetramethyl)isoindoline-1,3-dione (SI-2-4Cl)

Yield 75%; m.p. 230 $^{\circ}$C; ^{1}H NMR (CDCl$_3$, 400 MHz, δ ppm): 8.03 (s, 4H), 2.35 (s, 12H). FTIR (KBr) υ/cm^{-1}: 3120, 1777 and 1728 (imide). CHN Calculated for C$_{26}$H$_{16}$Cl$_4$N$_2$O$_4$ (562): C, 62.94; H, 3.22; N, 5.64. Found: C, 62.45; H, 2.98; N, 5.48.

4,4`-bis-(5,6-dichloro-1,3-dioxoisoindolin-4-yl)-3,3`,5,5`-tetramethylbenzidine-1,3-dione (SI-3-4Cl)

Yield 82%; m.p. 234 $^{\circ}$C; ^{1}H NMR (CDCl$_3$, 400 MHz, δ ppm): 8.07 (s, 4H), 7.07 (s, 4H), 2.35 (s, 12H). FTIR (KBr) υ/cm^{-1}: 3122, 1770 and 1733 (imide). CHN Calculated for C$_{32}$H$_{20}$F$_4$N$_2$O$_4$ (638): C, 67.13; H, 3.49; N, 4.89. Found: C, 66.84; H, 3.08; N, 4.28.

5,5`-bis-(5,6-dichloro-1,3-dioxoisoindolin-4-yl)-4,4`-hexafluoroisopropylidene-1,3-dione (SI-4-4Cl)

Yield 86%. m.p. 213 $^{\circ}$C; ^{1}H NMR (CDCl$_3$, 400 MHz, δ ppm): 8.12 (s, 4H), 7.52-7.49 (d, 4H), 7.13-7.10 (d, 4H). FTIR (KBr) υ/cm^{-1}: 3128, 1775 and 1748 (imide). CHN Calculated for C$_{29}$H$_{14}$Cl$_4$N$_2$O$_4$ (594): C, 65.90; H, 2.65; N, 5.30. Found: C, 65.34; H, 2.41; N, 4.98.

5,6-bis-(dichloro-1,3-dioxoisoindolin-2-yl)-2,2`-bis-trifluoromethylbenzidine-1,3-dione (SI-5-4Cl)

Yield 81%; m.p. 223 $^{\circ}$C; ^{1}H NMR (CDCl$_3$, 400 MHz, δ ppm): 8.08 (s, 4H), 7.62 (s, 2H), 7.13 (s, 2H), 2.35 (s, 6H). FTIR (KBr) υ/cm^{-1}: 3116, 1768 and 1736 (imide). CHN Calculated for C$_{32}$H$_{20}$Cl$_4$N$_2$O$_4$ (704): C, 60.21; H, 3.16; N, 4.39. Found: C, 60.13; H, 3.11; N, 4.31.

3,5-bis-(5,6-dichloro-1,3-dioxoisoindolin-1-yl)-9-methyleneanthracen-10(9H)-one-hydrate)isoindoline-1,3-dione (SI-6-4Cl)

Yield 70%; m.p. 244 $^{\circ}$C; ^{1}H NMR (CDCl$_3$, 400 MHz, δ ppm): 8.08 (s, 4H), 7.62 (s, 2H), 7.13 (s, 2H), 2.35 (s, 6H). FTIR (KBr) υ /cm^{-1}: 3116, 1768 and 1736 (imide). CHN Calculated for C$_{32}$H$_{20}$Cl$_4$N$_2$O$_4$ (638): C, 67.13; H, 3.49; N, 4.89. Found: C, 67.03; H, 3.11; N, 4.71.

5,6-dichloro-2-(6-(5,6-dichloro-1,3-dioxoisoindolin-2-yl)-pyridine)isoindoline-1,3-dione (SI-7-4Cl)

Yield 90%; m.p. 245 $^{\circ}$C; ^{1}H NMR (CDCl$_3$, 400 MHz, δ ppm): 8.08 (s, 4H), 7.13-7.18 (t, 1H), 5.92-7.98 (d, 2H). FTIR (KBr) υ/cm^{-1}: 3116, 1768 and 1736 (imide). CHN Calculated for C$_{21}$H$_7$Cl$_4$N$_3$O$_4$ (507): C, 57.14; H, 1.58; N, 9.52. Found: C, 57.03; H, 1.31; N, 9.13.

Synthesis of PIM-SIs

The microporous polymer PIM-SI-(1-7)s were prepared in good yield (80%) by the benzodioxane formation reaction between the corresponding difunctional monomers (1 and 2) as illustrated in Scheme 1. A mixture of monomer (SI-1-4F) (0.5 g, 0.90 mmol), TTSBI (0.6 g, 1.8 mmol) and K$_2$CO$_3$ (0.70 g, 5.4 mmol) in dry DMF (100 ml) was stirred at 120 $^{\circ}$C for 24 h. After cooling, the reaction mixture was poured into deionised water and the solid product collected by filtration and washed with methanol. The optained polymer was then purified by refluxing in *n*-hexane, acetone and chloroform. The obtained yellow powder PIM-SI-1 was dried in a vacuum oven at 100 $^{\circ}$C for 12 h (1.5 g, yield 85 %). Analysis by GPC (CHCl$_3$): Mn = 11,000, Mw = 38,000, Mw/Mn = 3.4. ^{1}H NMR (CDCl$_3$, 400 MHz, δ ppm): 1.39 (s, 12H), 2.34-2.36 (d, 4H), 6.6 (s, 4H), 7.18-7.21 (d, 4H), 7.61 (s, 2H). IR (KBr) υ/cm^{-1}: 1779 (asym C=O, str), 1727 (sym C=O, str), 1359 (C-N, str). CHN Calculated for the proposed repeat unit C$_{45}$H$_{30}$N$_2$O$_8$ (726): C, 74.38; H, 4.13; N, 3.85%; Found C, 73.68; H, 4.02.; N, 3.52. BET surface area = 397 m^2/g; total pore volume = 0.22 cm^3/g.

The following polymers were prepared from corresponding chloro-monomers using similar procedure adopted for PIM-SI-1.

PIM-SI-2

Yield 88%; m.p. >300 $^{\circ}$C. Analysis by GPC (CHCl$_3$): Mn = 19,000, Mw = 40,000, Mw/Mn = 2.2. ^{1}H NMR (CDCl$_3$, 400 MHz, δ ppm): 1.39 (s, 12H), 2.34-2.36 (d, 4H), 2.45 (s, 12H), 6.6 (s, 4H), 7.61 (s, 2H). IR (KBr) υ/cm^{-1}: 1781 (asym C=O, str), 1726 (sym C=O, str), 1360 (C-N, str). CHN Calculated for C$_{47}$H$_{36}$N$_2$O$_8$ (756): C, 74.60; H, 4.76; N, 3.70 %; Found C, 73.98; H, 4.32; N, 3.32. BET surface area = 619 m^2/g; total pore volume = 0.32 cm^3/g.

PIM-SI-3

Yield 78%; m.p. >300 $^{\circ}$C. Analysis by GPC (CHCl$_3$): Mn = 18,000, Mw = 39,000, Mw/Mn = 2.1. ^{1}H NMR (CDCl$_3$, 400 MHz, δ ppm): 1.39 (s, 12H), 2.34-2.36 (d, 4H), 2.45 (s, 12H), 6.45 (s, 4H), 7.12 (s, 4H), 7.55 (s, 2H). IR (KBr) υ/cm^{-1}: 1775 (asym C=O, str), 1725 (sym C=O, str), 1355 (C-N, str). Elemental analysis calcd (%) for the proposed repeat unit

$C_{53}H_{40}N_2O_8$ (832) requires C, 76.44; H, 4.80; N, 3.36 %; Found C, 75.91; H, 4.21; N, 3.02. BET surface area = 470 m²/g; total pore volume = 0.45 cm³/g.
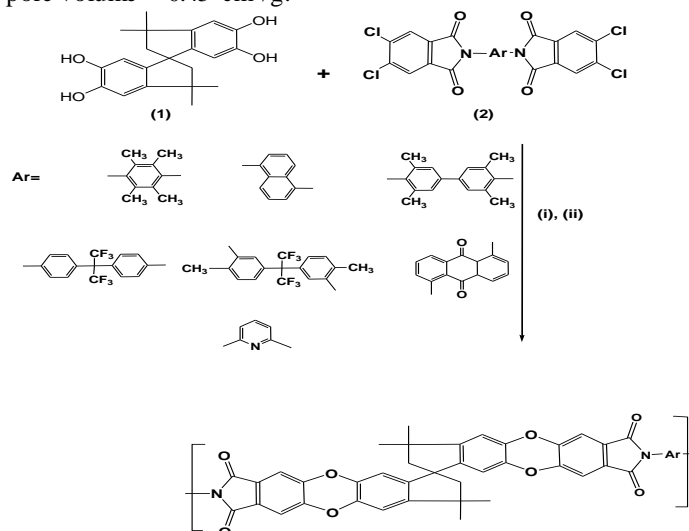
Scheme 1: Synthetic Pathway Toward the PIM-SI-(1-7)s. Reagents and Conditions: (i) K₂CO₃, (ii) DMF, 120 ℃ for 24h

PIM-SI-4

Yield 72%; m.p. >300 ℃. GPC: Mn = 33,000, Mw = 66,000, Mw/Mn = 2.0. ¹H NMR (CDCl₃, 400 MHz, δ ppm): 1.39 (s, 12H), 2.34-2.36 (d, 4H), 2.45 (s, 12H), 6.55 (s, 4H), 7.32 (s, 4H), 7.72 (s, 2H). IR (KBr) υ/cm⁻¹: 1781 (asym C=O, str), 1723 (sym C=O, str), 1357 (C-N, str). CHN Calculated for $C_{52}H_{32}N_2O_8F_6$ (926): C, 67.38; H, 3.45; N, 3.02%; Found C, 66.92.; H, 3.16; N, 2.71. BET surface area = 800 m²/g; total pore volume = 0.52 cm³/g.

PIM-SI-5

Yield 80%; m.p. >300 ℃. GPC: Mn = 19,000, Mw = 38,000, Mw/Mn = 2.0. ¹H NMR (CDCl₃, 400 MHz, δ ppm): 1.33 (s, 12H), 2.24-2.26 (d, 4H), 2.41 (s, 12H), 6.23 (s, 4H), 7.12 (s, 4H), 7.55 (s, 2H). IR (KBr) υ/cm⁻¹: 1780 (asym C=O, str), 1725 (sym C=O, str), 1368 (C-N, str). CHN Calculated for $C_{51}H_{30}N_2O_8$ (912): C, 67.10; H, 3.28; N, 3.07%; Found C, 66.71; H, 3.10; N, 2.90. BET surface area = 485 m²/g; total pore volume = 0.59 cm³/g.

PIM-SI-6

Yield 65%; m.p. >300 ℃. Mn = 10,000, Mw = 28,000, Mw/Mn = 2.8. ¹H NMR (CDCl₃, 400 MHz, δ ppm): 1.33 (s, 12H), 2.24-2.26 (d, 4H), 6.23 (s, 4H), 6.23-6.25 (d, 4H), 6.22-6.24 (t, 2H). IR (KBr) υ/cm⁻¹: 1778 (asym C=O, str), 1722 (sym C=O, str), 1361 (C-N, str). CHN Calculated for $C_{51}H_{30}N_2O_{10}$ (830): C, 73.73; H, 3.63; N, 3.37%; Found C, 73.20.; H, 3.39; N, 3.13. BET surface area = 415 m²/g; total pore volume = 0.65 cm³/g.

PIM-SI-7

Yield 82%; m.p. >300 ℃. Mn = 14,000, Mw = 35,000, Mw/Mn = 2.5. ¹H NMR (CDCl3, 400 MHz, δ ppm): 1.33 (s, 12H), 2.24-2.26 (d, 4H), 6.23 (s, 4H), 6.23-6.25 (d, 2H), 6.33-6.36 (t, 1H). IR (KBr) υ /cm⁻¹: IR (KBr) υ /cm⁻¹: 1777 (asym C=O, str), 1728 (sym C=O, str), 1363 (C-N, str). CHN Calculated for $C_{42}H_{27}N_3O_8$ (701): C, 71.89; H, 3.85; N, 5.99%; Found C, 71.33; H, 3.21; N, 5.35. BET surface area = 430 m²/g; total pore volume = 0.55 cm³/g.

Results and discussions

The phthalimide based chlorinated monomers (SI-4Cls) were prepared in good yield by the straight forward one step imidisation reaction between dichlorophthalic anhydride and different amines in refluxing acetic acid. The proposed structure and purity of the obtained chlorinated monomers were confirmed by routinely spectroscopic techniques as well as elemental analysis. The possibility of the preparation of ladder polymer was confirmed by making model compounds directly from a reaction between two molar equivalents of di-*tert*iarybutyl catechol with the different difchlorophthalimide (See Supporting Information). The reaction product was characterized by mass, ¹H NMR, FTIR spectroscopy and elemental analysis confirming that all the four F atoms were replaced by the two benzodioxane units. The highly efficient reaction (yield >90%) promotes the preparation of microporous organic polymers. The PIM-SIs polymers were synthesized by the dibenzodioxane formation reaction between the 5,5',6,6'-tetrahydroxy-3,3,3',3'-tetramethylspirobisindane (spirobiscatechol), and various fluorine-containing monomers (SI-4Cl) in dry DMF as illustrated in scheme 1.

The polymers were isolated by precipitation in acidified water and the resulting powder samples were purified by refluxing in deionised water, methanol and ethanol respectively followed by reprecipitation in a chloroform/methanol mixture to give yellow fluorescent powder in good yield (>85%) attributed to the efficiency of the polycondensation reaction. The solution processable PIM-SIs can be cast into membrane which can be used as a separation membrane, selectively removing one component either from liquid or gas mixture.

According to our previous experiments, we note that the synthesis of PIM-SIs having high molecular weight could be carried out at revised conditions especially elevated temperature and high concentration. After a number of trials, we found that the solvent DMF is significantly compatible with the reaction mixture to a great extent and could achieve high molecular weight linear polymers while compared to DMAc and NMP.

TTSBI is soluble in polar solvents such as THF, methanol, ethanol and insoluble in nonpolar solvents such as dichloromethane, chloroform, and *n*-hexane. As is the general tendency for phenols, TTSBI is easily oxidized by exposure to air during normal laboratory handling, for example; TTSBI solution in ethanol becomes yellow due to the oxidized impurities.

The solution became darker with increasing levels of impurities. It is crucial in condensation polymerization to use pure monomers to obtain polymers with high molecular weights. Therefore, to purify TTSBI monomer, a 10 g sample of it was dissolved in 80 g of hot methanol. Half of this solution was evaporated by heating, followed by adding of CH₂Cl₂ to the hot solution slowly until the solution become cloudy. The solution was allowed to stand for 2h. Then the resulting white solid was collected by vacuum filtration. Purified TTSBI was dried at 60 ℃ under vacuum for 2 days until there was no further weight reduction. In attempt to increase the reaction rate and molecular weight, the ratio of K₂CO₃ to TTSBI monomer, temperature, and solvent type were controlled. If the reaction temperature was 130 ℃ with a 24 h or longer, the resulting polymer was insoluble in THF or CH₂Cl₂, which indicated that cross-linking polymerization occurred. When the reaction temperature was decreased to 80 ℃ for same time, the resulting polymer was soluble in methanol, which indicated that its molecular weight was too low to precipitate in methanol.

When the reaction was conducted for 24 h and at temperature of 120 ℃, the resulting polymer had high molecular

weight. This temperature was then selected for studying the effects of the K_2CO_3 concentration. The polymerization temperature at 120 ºC and higher monomer concentrations (monomer to solvent ratio 1 mmol: 2 ml) in DMF were used. In addition, the using of the following solvent system (toluene: DMF in ratio of 1:8 V/V respectively) was introduced into the reaction not only to remove generated water, but also to provide solubility enhancement of the polymer.

Oligomers and Cyclic Polymers Removal

Due to the nature of this reaction, it is difficult to prevent the formation of oligomer and cyclic polymers, their presence being inferred from GPC curves. Used a process of repeated reprecipitation from methanol to remove these oligomers and cyclic polymers which is tedious and costly.[17] A convenient and simplified method for purification was developed as follows: when a 1-2 fold amount (volume over DMF) of THF was added to the reaction flask after the reaction was terminated, the dispersed linear polymer particles coagulated and precipitated at the bottom of the reaction flask.[18] This method preferentially coagulates high molecular weight polymer and removes low molecular weight fractions. The oligomers and cyclic polymers were soluble in the mixture of THF and DMF. In some cases, when the resulting polymer had low molecular weight, no precipitate formed in the mixture of THF and DMF. In common with all phenolics, we make the assumption that some phenol groups in TTSBI are susceptible to oxidation into a benzoquinone-type structure (Scheme 2).[19] Polymerization in corporating oxidized TTSBI would lead to single-bond chain defects and unreacted florine groups in the ladder polymer. This residual (–Cl) is amenable to reaction with phenolate chain ends of another PIMs chain, resulting in branched or crosslinked structures.
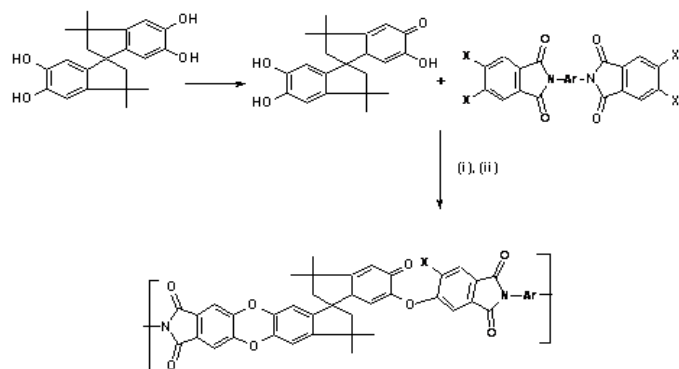
Scheme 2: Possible Chain Defects Leading to Branching or Cross-Linking PIMs during Condensation Polymerization.[19] Reagents and Conditions: (i) Dry DMF, Anhydrous K_2CO_3, and (ii) 120 ºC for 24 h

Nitrogen Gas Adsorption Analysis

Nitrogen adsorption/desorption isotherms at 77 K were investigated for PIM-SI-(**1-7**)s. Apparent surface areas, was calculated from N_2 adsorption isotherms using (BET) method. The nitrogen adsorption/desorption isotherms for PIM-SI-**2** (Figure 1) shows type I in shape and a high N_2 uptake at very low relative pressure with completely reversible. From the porosity analysis (Figure 2) it is clear that the prepared polymers are analogous to polymers of intrinsic microporosity (PIMs) with high surface area (415-619 m²/g). The PIMs exhibit pronounced hysteresis, the N_2 desorption curve lying above the adsorption curve, with the hysteresis extending down to low relative pressures. Low pressure hysteresis like this has occasionally been observed for other microporous materials, and

may be attributed either to sorbate-induced swelling or to a complex micropore structure with throats and cavities. In PIM-SIs, for which the microporosity arises from a complex distribution of interconnected free volume, it is likely that the low pressure hysteresis arises preimarily from the presence of constrictions. However, swelling effects may also play a role and this may be particularly significant in the PIM-SI-**1**, and PIM-SI-**6** for which the hysteresis is large. The hysteresis is high in case of linear polymer containing anthraquinon and naphthalene unit as PIM-SI-**1** and PIM-SI-**6**. The bulk groups in PIM-SI-(**1 and 6**) are likely to decrease the interdigitation and allow greater swelling of the network during N_2 adsorption.[20] The hysteresis of the N_2 isotherm of PIM-SI-(**4 and 5**) is relatively small which may be due to the strong dipolar interactions between interdigitated -CF_3 groups in different layers reducing swelling effect.
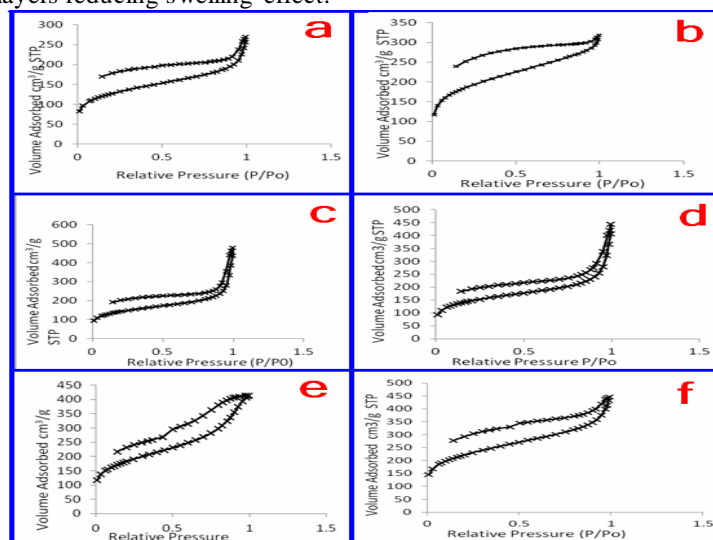
Figure 1: Nitrogen adsorption and desorption at 77 K for (a) PIM-SI-6, (b) PIM-SI-1, (c) PIM-SI-4, (d) PIM-SI-5, (e) PIM-SI-3, and (f) PIM-SI-7

Hydrogen gas Adsorption Analysis

The impressive hydrogen adsorption capacity of PIM-SIs is related to a high concentration of subnanometre micropores, as verified by (HK) and (NLDFT) analyses of low-pressure nitrogen adsorption data. Figure 2 and 3 shows the micropore size distribution for PIM-SI-4 polymer sample as calculated by the (HK) and NLDFT methods. This linear polymer shows relatively broad distribution with a maximum of 0.62 nm. The hydrogen adsorption/desorption of PIM-SI-5 and PIM-SI-6 are shown in Figures 4 and 5.
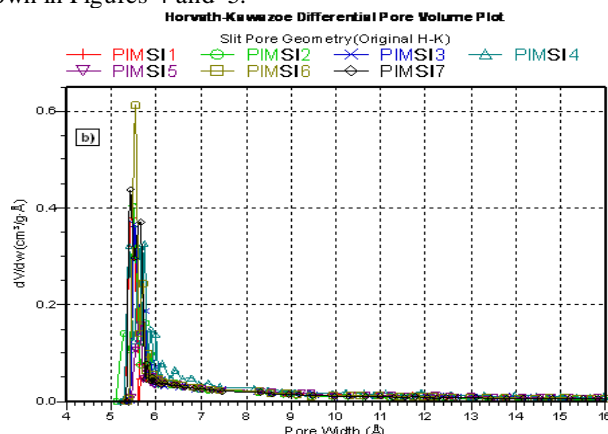
Figure 2: Horvath-Kawazoe Differential Plot for PIM-SIs at 77 K
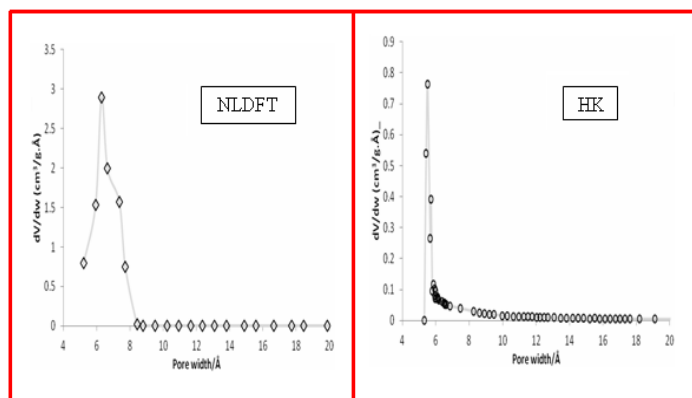
Figure 3: Micropore size distributions calculated using NLDFT and HK methods for PIM-SI-4
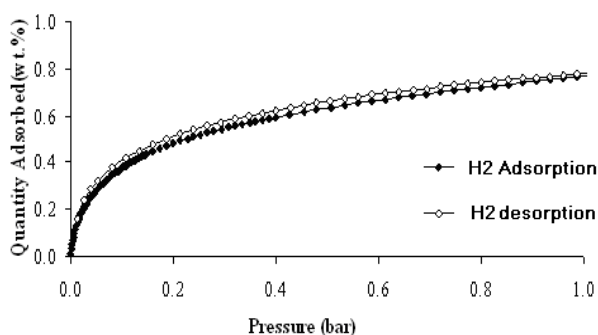
Figure 4: Hydrogen adsorption/desorption isotherm of PIM-SI-5 at 77 K
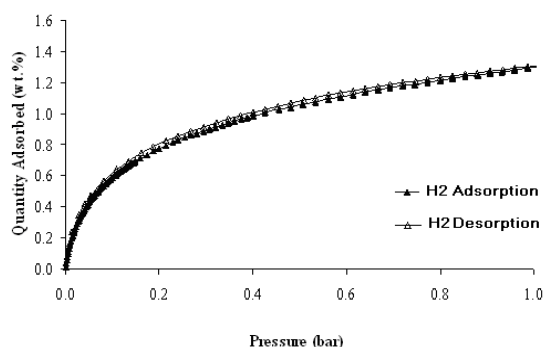
Figure 5: Hydrogen adsorption/desorption isotherm for PIM-SI-6 at 77 K

From the isotherms, it was found that there were no kinetic trapping of hydrogen in small pores upon desorption. The Hydrogen adsorption capacities by various samples with different surface areas usually reveal a linear relationship between BET surface area and H_2 storage capacity at low pressure.

For example the H_2 adsorption capacity of PIM-SI-**1** (0.79 wt.%) and PIM-SI-**6** (1.18 wt.%) at 1 bar and 77 K with their BET surface areas 595 and 889 m^2/g respectively, is consistent with the above hypothesis.

Thus from the comparison of various synthesised PIM-SI, the H_2 adsorption capacities are largely influenced by BET surface area as shown in Figure 6. Several studies showed that a clear relationship exist between total surface area and hydrogen adsorption density of porous material.[21-23]

The hydrogen adsorption at 77 K, physisorption mechanism is dominant and the H_2 uptake is controlled by the structural features of the adsorbent material. Moreover small micropores can effectively adsorb hydrogen, probably due to its much

smaller kinetic diameter compared to bigger gas molecules such as N_2.
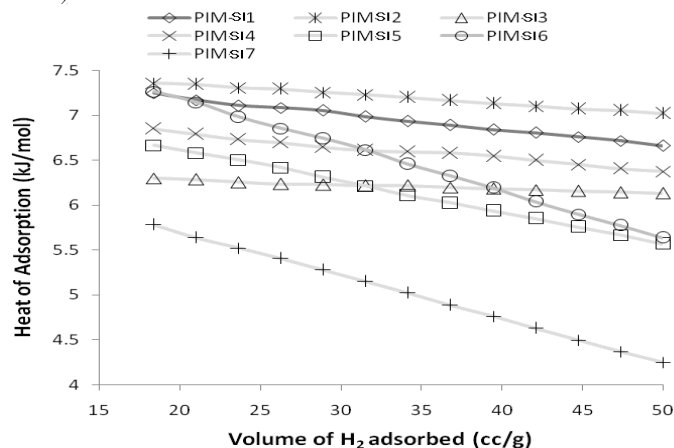
Figure 6: Isoteric Heat of Hydrogen Adsorption for PIM-Sis Calculated Using Adsorption Isotherms at 77 and 87 K

Film Characterization

The thicknesses of the PIM-Sis films were tested in the choice between 50 and 80 μm. The samples were weighed on analytical balance and their densities were calculated using the known sample area and thickness. The densities ranged from 1.07 to 1.09 g/cm^3, essentially identical to values previously reported by P. M Budd et al.[24-25] Trifluoromethyl groups (-CF_3) in PIM-SI-(**4** and **5**) significantly improve permeability and selectivity by increasing chain stiffness and reducing interchain interactions.[26] Also (-CF_3) side groups acts favorably to increase polymer solubility. In addition, the rigidity of the ladder polymer chain with (-CF_3) groups can be enhanced by hindering bond distortion within the ladder chain.[27-28] SI-**3** monomer contains a longer linker and probably less stiff than SI-**2** monomer due to the single bond of the biphenyle. SI-**4** is also along linker and introduces an additional kink into the polymer chain. The difference in chemical structural compositions, and pore sizes between PIM-SI-**4** (left) (from fluorinated starting material) and PIM-SI-**4** (right) (from chlorinated starting material) films is consistent with the different physical appearance as shown in Figure 7 of the two porous films, i.e. PIM-SI-**4** films are good flexibility, transparency, and the strong thin films, while chlorinated film of same monomers are less flexible opaque and self stable films. The new developed polymers promise to become high-performance polymers for microelectronic, optical, and semiconductor applications.[29-35]

Figure 7: Left: PIM-SI-4 from Fluorinated Starting Material, While RIGHT: PIM-SI-4 from Chlorinated Starting Material 4

GPC Analysis

The weight average molecular weights of PIM-SI-(**1-7**) were recorded in the range of 2.8- 4.4×10^4 g/mol based on polystyrene standard. Molecular weights and molecular weight

distributions were determined by (GPC), for example, GPC of PIM-SI-**5** shows Mn of 19000 and Mw of 38000 as shown in Figure 8. The data obtained by GPC for PIM-SIs are different, since the chemical and structural composition and degree of polymerization of the used standard PIM-SIs are different.
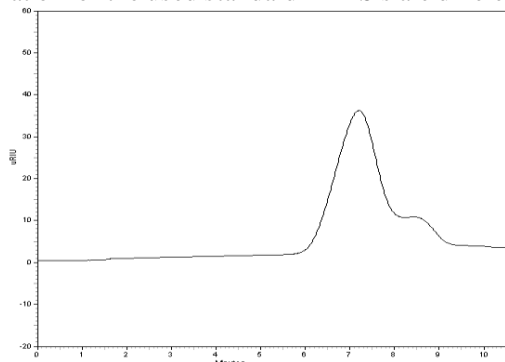
Figure 8: GPC Traces of PIM-SI-4 in CHCl₃ Against PS Standard

All the polymers have polydispersities between 2.0 and 3.4 (the average molecular weight distributions were generally moderate (PDI ≈ 2.5). Generally, the Mw of the PIM-SI-**4** was higher than the other PIM-SIs. This become also obvious when polymer films were cast, on which PIM-SI-4 gave stable film, while no free-standing films could be formed from PIM-SI-(**1**, **3**, **6**, and **7**). The obtained low molecular weights of the PIM-SI-**6** and PIM-SI-**1** might be explained by geometric arguments. Nevertheless, the polymer was fractionated using selective precipitation in a chloroform/methanol mixture. The original product showed a shoulder at an elution volume at about 8 min, this shoulder which could be returned to a relatively low molecular weight compound again as a pronounced peak in the first fraction.

The following polymers PIM-SI-**2**, PIM-SI-**3**, PIM-SI-**4**, PIM-SI-**5** and PIM-SI-**7** has obtained with molecular weight (Mw between 33,000 and 42,000) (as shown in Table **1**). The polymer prepared from SI-**4** and SI-**5** monomers had the highest Mn. A plausible explanation is that the –CF₃ group enhance the solubility of the polymer and growing chain, which result unfolded, uncoiled, unpacked chains with facilitated growing.

Table 1: ᵃNumber-Average Molar Mass, Mn, Weight-Average Molar Mass, Mw/Mn, Determined by GPC. ᵇBET Surface Area, SA$_{BET}$ Determined from N₂ Adsorption at 77 k

PIMs	M_n(g mol⁻¹)ᵃ	M_w(g mol⁻¹)ᵃ	M_w/M_n	SA$_{BET}$ (m²/g)ᵇ	PV$_{micro}$ (Cm³/g)
PIM-SI-1	9000	36000	3.4	585	0.21
PIM-SI-2	17000	38000	2.2	607	0.30
PIM-SI-3	16000	37000	2.1	458	0.42
PIM-SI-4	31000	42000	2.0	463	0.50
PIM-SI-5	17000	36000	2.0	473	0.57
PIM-SI-6	8000	26000	2.8	403	0.61
PIM-SI-7	12000	33000	2.5	418	0.53

Conclusions

In conclusion, a new series of linear phthalimide based organic polymers were synthesized by the nucleophilic substitution reaction using cheaper various chloro-monomers (instead of fluoro-monomers) and 5,5',6,6'-tetrahydroxy-3,3,3',3'-tetramethylspirobisindane. The FT-IR, ¹H NMR, and elemental analyses indicated that the polymers appear to have the same proposed structure. The pore size distribution analysis shown that pores are narrowly distributed and fine-tuned with a subnanometer dimension, The intrinsic microporosity of these polymers is supported by good hydrogen uptake at 77 K and 87 K. Isosteric heat of H₂ adsorption (Q$_{st}$) measurement revealed that Q$_{st}$ is not highly sensitive to the structural features and exhibit high isoteric heats of adsorption up to 8.49 kJ/mol.

References
1. Lee, J-Y.; Wood, C. D.; Bradshaw, D.; Rosseinky M. J.; Cooper, A. I. Chem Commun 2006, 2670-2672; Wood, C. D.; Tan, B.; Trewin, A.; Niu, H.; Bradshaw, D.; Rosseinsky, M. J.; Khimyak, Y. Z.; Campbell, N. L.; Kirk, R.; Stockel E. and Cooper, A. I. Chem Mater 2007, 19, 2034-2048.
2. a) Germain, J.; Hradil, J.; Frechet, J. M. J.; Svec, F. Chem Mater 2006, 18, 4430-4435; b) Germain, J.; Svec F.; and Frechet J. M. J. Chem Mater 2008, 20, 7069–7076.
3. Ghanem, B. S.; McKeown, N.B.; Harris, K.D.M.; Pan, Z.; Budd, P.M.; Butler, A.; Selbie, J.; Book D.; Walton, A. Chem Commun 2007, 67-69.
4. Jiang, Jia-X.; Su, F.; Trewin, A.; Wood, C. D.; Campbell, N. L.; Niu, H.; Dickinson, C.; Ganin, A.Y.; Rosseinsky, M. J., Khimyak Y.Z.; Cooper A.I. Angew Chem Int Ed. 2007, 44, 8574–8578.
5. Makhseed S.; Samuel. J. Chem Commun 2008, 4342- 4344.
6. Yuan, S.; Dorney, B.; White, D.; Kirklin, S.; Zapol, P.; Yu, L.; Liu, Di-J. Chem Commun 2010, 46, 4547- 4549.
7. Wang, Z.; Zhang, B.; Yu, H.; Sun, L.; Jiao, C.; Liu, W. Chem Commun 2010, 46, 7730-7732.
8. McKeown N. B.; Budd P. M. Chem Soc Rev 2006, 35, 675-683.
9. a) Budd, P. M.; Ghanem, B. S.; Makhseed, S.; Mckeown, N. B.; Msayib, K.; Tattershall, C. E.; Wang, D. Chem Commun 2004, 2, 230-231; Budd, P.M.; Elabas, E.S.; Ghanem, B.S.; Makhseed, S.; McKeown, N.B.; Msayib, K.J.; Tattershall, C.E.; Wang, D. Advanced Mater 2004, 16, 456-459; McKeown, N. B.; Budd, P. M.; Msayib, K.; Ghanem, B. S.; Kingston, H. J.; Tattershall, C. E.; Makhseed, S.; Reynolds, K. J.; Fritsch, D. Chemistry- A European J. 2005, 11, 2610-2620.
10. Yongli Mi. Takuji Hirose. Journal of polymer research, 1996, 3, 11-19.
11. Y. H. Kim, H. S. Kim, S. K. Kwon. Macromolecules, 2005, 38, 7950–7956.
12. J. Li, J. Kato, K. Kudo, S. Shiraishi. Macromol. Chem. Phys., 2000, 201, 2289–2297.
13. Yuan H., Jui-Ming Y., Shir-Joe L., Yen-P C. Acta Materialia, 2004, 52, 475-486.
14. Z.M. Qiu, J.H. Wang, Q.Y. Zhang, S.B. Zhang, M.X. Ding, L.X. Gao. Polymer, 2006, 47, 8444-8452.
15. Y. Tsuda, T. Yoshida, T. Kakoi., Polymer, 2006, 38, 88–90.
16. Quanyuan Z., Guang C., Suobo. Z. Polymer. 2007, 48, 2250-2256.
17. Wang Q, Luo J, Zhong Z, Borgna A. *Energy Environ Sci*, 2011, 4, 42–55.
18. J.G. Wijmans, C.A. Smolders. European Polymer Journal, 1983, 19, 1143–1146.
19. J. Song, N. Du, G. P. Robertson, Y. Dai, M. D. Guiver, S. Thomas, I. Pinnau. Macromol, 2008, 41, 7411-7417.
20. J. P. Cotton, D. Decker, H. Benoit, B. Farnoux, J. Higgins, G. Jannink, R. Ober, C. Picot, J. des Cloizeaux. Macromolecules. 1974, 7, 863–872.
21. Dinca, M.; Yu, A. F.; Long, J. R. J. Am Chem Soc 2006, 128, 17153–17153.

22. Foy, A.G.W.; Matzger A.J.; Yaghi, O.M. J. Am Chem Soc 2006, 128, 3494–3495.

23. Mckeown, N.B.; Gahnem, B.; Msayib, K.J.; Budd, P.M.; Tattershall, C.E.; Mahmood, K. Angew Chem Int Ed. 2006, 45, 1804–1807.

24. P. M Budd, N. B. Mckewn, D. Fritsch. Macromol. 2006, 245, 403-405.

25. N. Du, G.P.Robertson, J. Song, I. Pinnau, S. Thomas. *Macromol*, 2008, 41, 9656-9662.

26. Jens Weber, Naiying Du, Michael. D. Macromolecules. 2011, 44, 1763-1767.

27. B.Y. Liu, W. Hu, T. Matsumoto, Z.H. Jiang, S. Ando. J. Polym. Sci., Part A: Polym. *Chem.*, 2005, 43, 3018-3029.

28. T. Matsuura, S. Ando, S. Sasaki; et al., Macromolecules, 1994, 27, 6665-6670.

29. L.J. Markoski, D.S. Thompson, J.S. Moore. Macromolecules, 2000, 33, 5315-5317.

30. J. Seo, S.Y. Lee, W. Jang, H. Han. J. Appl. Polym. Sci., 2003, 89, 3442-3446.

31. J. Seo, H. Han. Polym. Degrad. Stabil., 2002, 77, 477- 482.

32. M. Ree, T.J. Shin, Y.H. Park, S.I. Kim, S.H. Woo, C.K. Cho, C.E. Park.. J. Polym. Sci. Part B: Polym Phys., 1998, 36, 1261-1273.

33. S. Ando., J. Photopolym. Sci. Technol., 2004, 17, 219-232.

34. J. Jagur-Grodzinski, (2007). Polymeric materials for fuel cells: concise review of recent studies, *Polym. Adv. Technol*., **18**, 785–799.

35. S. Möller, C. Perlov, W. Jackson, C. Taussig, S.R. Forrest1. Nature, 2003, 426, 166-169.